

GRB 011121: A Massive Star Progenitor

P. A. Price^{1,2}, E. Berger², D. E. Reichart², S. R. Kulkarni², R. Subrahmanyan³, R. M. Wark³, M. H. Wieringa³, D. A. Frail^{4,2}, J. Bailey⁵, B. Boyle⁵, E. Corbett⁵, K. Gunn⁶, S. D. Ryder⁵, N. Seymour⁶, K. Koviak⁷, P. McCarthy⁷, M. Phillips⁷, T. S. Axelrod¹, J. S. Bloom², S. G. Djorgovski², D. W. Fox², T. J. Galama², F. A. Harrison², K. Hurley⁸, R. Sari², B. P. Schmidt¹, S. A. Yost², M. J. I. Brown⁹, T. Cline¹⁰, F. Frontera¹¹, C. Guidorzi¹² and E. Montanari¹².

ABSTRACT

Of the cosmological gamma-ray bursts, GRB 011121 has the lowest redshift, $z = 0.36$. More importantly, the multi-color excess in the afterglow detected in the Hubble Space Telescope (HST) light curves is compelling observational evidence for an underlying supernova. Here we present near-infrared and radio observations of the afterglow. We undertake a comprehensive modeling of these observations and those reported in the literature and find good evidence favoring a wind-fed circumburst medium. In detail, we infer the progenitor had a mass loss rate of $\dot{M} \sim 10^{-7}/v_{w3} M_{\odot} \text{ yr}^{-1}$ where v_{w3} is the speed of the wind from the progenitor in units of 10^3 km s^{-1} . This mass loss rate is similar to that inferred

¹Research School of Astronomy & Astrophysics, Mount Stromlo Observatory, via Cotter Road, Weston, ACT, 2611, Australia.

²Palomar Observatory, 105-24, California Institute of Technology, Pasadena, CA, 91125.

³Australia Telescope National Facility, CSIRO, P.O. Box 76, Epping NSW 1710, Australia.

⁴National Radio Astronomy Observatory, P.O. Box O, Socorro, NM, 87801.

⁵Anglo-Australian Observatory, P.O. Box 296, Epping, NSW 1710, Australia.

⁶Department of Physics and Astronomy, University of Southampton, Highfield, Southampton SO17 1BJ, United Kingdom.

⁷Carnegie Observatories, 813 Santa Barbara Street, Pasadena, CA 91101.

⁸University of California Space Sciences Laboratory, Berkeley, CA, 94720.

⁹National Optical Astronomy Observatory, P.O. Box 26732, Tucson, AZ, 85726.

¹⁰NASA Goddard Space Flight Center, Code 661, Greenbelt, MD 20771.

¹¹Istituto Tecnologie e Studio Radiazioni Extraterrestri, CNR, Via Gobetti 101, 40129 Bologna, Italy.

¹²Dipartimento di Fisica, Universita di Ferrara, Via Paradiso 12, 44100, Ferrara, Italy.

for the progenitor of SN 1998bw which has been associated with GRB 980425. Our data, taken in conjunction with the HST results of Bloom *et al.* (2002), provide a consistent picture: the long duration GRB 011121 had a massive star progenitor which exploded as a supernova at about the same time as the GRB event.

Subject headings: gamma rays: bursts

1. Introduction

On 2001 November 21 at 18:47:21 UT, GRB 011121 was detected and localized by the Italian-Dutch satellite BeppoSAX (Piro 2001). The localization was further improved by the InterPlanetary Network (Hurley *et al.* 2001) and an optical transient was identified by the OGLE group (Wyrzykowski, Stanek & Garnavich 2001). Spectroscopy of the transient revealed emission lines interpreted as arising from the host galaxy at a redshift of $z = 0.36$ (Infante *et al.* 2001).

Low redshift GRBs are particularly valuable in uncovering the origin of GRBs. If GRBs result from the death of massive stars then it is reasonable to expect an underlying supernova (SN). Bloom *et al.* (1999) attributed a late-time red excess seen in the afterglow emission of GRB 980326 to an underlying SN. This result triggered searches for similar excesses with no clear success save GRB 970228 (Reichart 1999; Galama *et al.* 2000). The low redshift is critical to such searches since the SN contribution is expected to exhibit strong absorption below 4000 Å (see Bloom *et al.* 1999).

Given this motivation, we triggered a sequence of multi-color and multi-epoch Wide Field and Planetary Camera 2 (WFPC-2) observations with the *Hubble Space Telescope* (HST). Garnavich *et al.* (2002) noted that the *R*-band flux of the first epoch of the HST observations was significantly in excess of the extrapolation of the power law decay of the early ground-based optical afterglow and attributed this to an underlying SN component. In Paper I (Bloom *et al.* 2002) we presented four-epoch multi-color HST light curves and show the data are explained by an underlying SN similar to SN 1998bw (Galama *et al.* 1998) except fainter by about 2/3 magnitude. At this point, there appears to be compelling evidence for GRB 011121 to be associated with a SN which exploded at about the same time as the gamma-ray event (Bloom *et al.* 2002).

This GRB-SN link is an essential expectation in the collapsar model (Woosley 1993) in which GRBs result from the death of certain massive stars. Another essential consequence of any massive star origin for GRBs, as noted by Chevalier & Li (1999), is a circumburst medium

fed by the inevitable and copious mass loss suffered by massive stars throughout their lives. Afterglow observations are excellently suited to determining not only the geometry of the explosion but also the distribution of circumburst matter. Unfortunately, until now there has been no clear evidence for a wind-fed circumburst medium (density, $\rho \propto r^{-s}$ with $s \sim 2$; here r is the distance from the explosion site) in the afterglow of any cosmologically located GRB.

Here we report near-infrared (NIR) and radio observations of the afterglow of GRB 011121. We undertake afterglow modeling of this important event and to our delight have found a good case for a wind-fed circumburst medium. Thus, the totality of the data — the HST optical lightcurves and multi-wavelength (radio, NIR, and optical) data — now support a massive star origin for this GRB.

2. Observations

Gamma-Rays: GRB 011121 was observed by numerous spacecraft in the InterPlanetary Network: Ulysses, BeppoSAX (GRBM), HETE-2 (FREGATE), Mars Odyssey (HEND) and Konus-Wind. The T_{90} duration, as determined from the Ulysses data, was 28 s, placing this event in the class of "long bursts" (Figure 1). The peak flux in the 25–100 keV range, over 0.25 s, was 2.4×10^{-6} erg cm $^{-2}$ s $^{-1}$, and the fluence was 2.4×10^{-5} erg cm 2 .

Near-Infrared: We observed the afterglow in the near-infrared with the newly-commissioned IRIS2 on the Anglo-Australian Telescope (AAT), WFIRC on the du Pont 2.5-m telescope and the IRCam on the Walter Baade 6.5-m telescope in J and K_s filters. The images were dark-subtracted, flat-fielded, sky-subtracted and combined using DIMSUM (Eisenhardt *et al.* 1999) in IRAF. PSF-fitting photometry of the afterglow using DAOPHOT (Stetson 1987) was performed relative to point sources in the field. Our multiple calibrations are consistent with each other and we estimate the systematic error to be less than 0.05 mag (see Table. 1).

Radio: We initiated observations of GRB 011121 with the Australia Telescope Compact Array (ATCA) starting on 2001 November 22.58 UT (see Table 2). The data were reduced and imaged using the Multichannel Image Reconstruction, Image Analysis and Display (MIRIAD) software package.

3. Modeling the Afterglow

3.1. Dust Extinction

In Figure 2 we display the optical/NIR spectrum of GRB 011121. The apparent curvature in the spectrum indicates a large magnitude of dust extinction. In view of this, estimating the dust extinction accurately is critical not only for the afterglow modeling but also as an important input parameter for the supernova modeling of the HST lightcurves (Bloom *et al.* 2002).

From the IR dust maps (Schlegel, Finkbeiner & Davis 1998) we estimate $A_V \approx 1.6$ mag. However, the IR maps have low angular resolution. Indeed, it appears that the line-of-sight to the afterglow passes through the edge of a dust cloud ~ 45 arcmin in extent. Fortunately, the availability of both the optical and NIR afterglow data allow us to directly estimate the extinction along this line of sight directly.

We make the reasonable assumption that the optical/NIR afterglow follows the standard power-law model, $F_\nu \propto t^{-\alpha}\nu^{-\beta}$, and we apply the parametric extinction curves of Cardelli, Clayton & Mathis (1989) and Fitzpatrick & Massa (1988) along with the interpolation suggested by Reichart (2001). Thanks to the abundance of our NIR data, which suffers little extinction, we can break the degeneracy between β and the magnitude of the extinction, A_V .

In addition to our own measurements we have included those reported in the literature (and noted in Figure 2). Since late-time measurements are increasingly dominated by an uncertain mix of the afterglow, the host galaxy and the nearby star B (Bloom *et al.* 2002) we restrict the analysis to data obtained over the first two days.

Our best fit has an unacceptable $\chi^2 = 66$ for 48 degrees of freedom, but this is mainly dominated by outliers, particularly in the data from the AAT where the seeing blended star B with the afterglow in some observations. Inserting an additional 3% error decreases the χ^2 to match the number of degrees of freedom. The additional error term, while *ad hoc*, is reasonable given the variety of telescopes and reduction techniques in our data set.

Our measured extinction is $A_V = 1.16 \pm 0.25$ mag, distinctly lower than that deduced from the dust maps. The type of extinction curve (e.g., Milky Way, LMC, SMC etc.) is unconstrained by these observations. We have not solved for extinction within the host galaxy, but the off-center location of the GRB (Bloom *et al.* 2002) makes it likely that the contribution from extinction within the host galaxy is small. Finally, we measure $\alpha = 1.66 \pm 0.06$ and $\beta = 0.76 \pm 0.15$, without assuming any specific afterglow model.

3.2. Afterglow Models

Armed with α and β we now consider three afterglow models: (i) isotropic expansion into a homogeneous medium (Sari, Piran & Narayan 1998), (ii) isotropic expansion into a wind-stratified medium (Chevalier & Li 1999), and (iii) collimated expansion into a homogeneous or wind-stratified medium (Sari, Piran & Halpern 1999). The models can be distinguished by a closure relation, $\alpha + b\beta + c = 0$. These closure relations are due to the dependence of both α and β on the electron energy distribution index, p , and the values of b and c depend on the location of the cooling frequency, ν_c , relative to the optical/NIR frequency, ν_O , at the epoch of the observations.

As can be seen from Table 3, models with isotropic expansion into an homogeneous medium (or, equivalently, a jet which becomes apparent on a timescale longer than the epochs of the optical/NIR data used here, $t_j \gtrsim 2$ d) are ruled out by the closure relations at more than 2σ significance. Two models produce closure consistent with zero: (*A*) A wind model with $\nu_c > \nu_O$ (effective epoch day 1), and $p = 2.55 \pm 0.08$; and (*B*) A fully developed jet at the time of the first optical observation, $t_j < 0.5$ d, with $\nu_c < \nu_O$ and $p = 1.66 \pm 0.06$.

The radio measurements, however, do not show any sign of a decay until at least ~ 7 days after the burst (Figure 3). The rising centimeter-band flux prior to this time indicates that the jet break is not at early times, and hence model *B*, the jet model, is ruled out. This then leaves us with model *A*, the wind model.

3.3. A Wind Model

The multi-wavelength data, radio through optical, can only be analyzed by considering the evolution of the broad-band synchrotron spectrum. In addition to ν_c , p and A_V we need to consider the self-absorption frequency, ν_a , and the peak frequency, ν_m , as well as the peak flux, $F_{\nu,m}$. These parameters are estimated from the data and can be inverted to yield physical quantities, i.e. the energy of the fireball, the density of the ambient medium, and the fractions of energy in the electrons, ϵ_e , and magnetic field, ϵ_B . An example of this approach can be found in Berger *et al.* (2001). The density in the wind model is parameterized by A_* , which is defined through $A = \dot{M}/4\pi v_w = 5 \times 10^{11} A_* \text{ g/cm}$ (see Chevalier & Li 1999) where v_w is the wind speed and \dot{M} is the mass loss rate. The normalization of $A_* = 1$ applies for a typical Wolf-Rayet wind speed of 10^3 km/sec and $\dot{M} = 10^{-5} M_\odot/\text{yr}$.

Given the sparse data we prefer to undertake the model fitting in an evolutionary approach rather than performing a blind χ^2 minimization search. For example, we fix the value of p and A_V to that determined earlier since the radio data has little bearing on these pa-

rameters. Next, we know that $\nu_c > \nu_O$, but there are no data in the X-ray band to actually constrain the value of ν_c . We therefore use $\nu_c \approx 10^{15}$ Hz since this is effectively the lowest value the cooling frequency can have in this model. We will, at a later point, revisit this issue and examine the consequences of increasing ν_c .

The remaining free parameters¹³, ν_a , ν_m , and $F_{\nu,m}$ are relatively easy to constrain for the following reasons. The value of $F_{\nu,m}$ determines the overall scaling in both the optical/NIR and radio bands, and is therefore constrained by two sets of data. The value of ν_m is constrained by the turnover in the radio lightcurves (at $t \approx 7$ days; see Figure 3), as well as the flux density of the optical/NIR lightcurves, since for a given value of $F_{\nu,m}$, the flux density in the optical/NIR band is determined by ν_m .

Finally, ν_a is constrained by the spectral slope between the two centimeter bands. The comparable flux between 4.8 and 8.7 GHz suggests that $\nu_a < 4.8GHz$. An independent constraint on ν_a is also provided by the equation due to Sari & Esin (2001):

$$C = 0.06(1+z)^4 t_{\text{day}}^4 d_{L,28}^{-2} \eta \left(\frac{\nu_a}{\text{GHz}} \right)^{10/3} \left(\frac{\nu_m}{10^{13} \text{ Hz}} \right)^{13/6} \left(\frac{\nu_c}{10^{14} \text{ Hz}} \right)^{3/2} \left(\frac{F_{\nu,m}}{\text{mJy}} \right)^{-1} \leq 0.25. \quad (1)$$

where $\eta = \min[(\nu_c/\nu_m)^{-(p-2)/2}, 1]$ is the fraction of the electron energy radiated away.

We find $F_{\nu,m} \approx 3$ mJy, $\nu_c \approx 10^{15}$ Hz, $\nu_m \approx 2 \times 10^{12}$ Hz, $\nu_a \approx 1.4$ GHz and $\eta = 0.2$ provide an adequate description of the afterglow data. From these parameters we obtain $A_* \sim 0.01$ and that inverse Compton cooling is marginally important. Higher values of A_* are possible in the inverse Compton-dominated regime and if $C \ll 1$, implying that ν_a is well below the centimeter bands. With these observations, we are unable to constrain such a model.

4. Discussion & Conclusions

GRB 011121, a relatively nearby burst ($z = 0.36$), has shot to fame given what appears to be firm identification of an underlying supernova component (Bloom *et al.* 2002). Here we presented early time NIR and comprehensive dual-frequency cm-wave observations of the afterglow. Thanks to the NIR data, we have been able to accurately measure the considerable Galactic extinction towards the burst, $A_V = 1.16 \pm 0.25$ mag, significantly smaller than that derived from extrapolations of the IR maps (Schlegel, Finkbeiner & Davis 1998). Our value

¹³Unless otherwise stated, all time-dependent parameters are evaluated at epoch 1 day e.g. $\nu_m \equiv \nu_m(t = 1 \text{ d})$.

of A_V is an important physical parameter in the modeling of the underlying SN component (Bloom *et al.* 2002).

If indeed long duration gamma-ray events such as GRB 011121 are linked to SNe then the progenitors of GRBs are massive stars. Such stars possess strong winds and one expects to see a signature of the wind-fed circumburst medium (Chevalier & Li 1999). The optical/NIR data alone rule out an isotropic explosion in a constant circumburst medium model. The radio data firmly rule out a model in which a jet is fully-developed at $t < 0.5$ d, but allow for a wind-fed circumburst medium. We estimate the mass loss rate, $\dot{M} \lesssim 10^{-7} v_{w3}^{-1} M_{\odot} \text{yr}^{-1}$ where v_{w3} is the wind speed in units of 10^3 km s^{-1} . In the collapsar model (MacFadyen, Woosley & Heger 2001), one expects the progenitors of GRBs to be massive stars which have lost their hydrogen envelopes, i.e. Wolf-Rayet stars. For such stars, $v_w \sim 10^3 \text{ km s}^{-1}$.

Interestingly enough, this mass loss rate is similar to that inferred for the progenitor of the Type Ic SN 1998bw, $2.5 \times 10^{-7} M_{\odot} \text{yr}^{-1}$ (Li & Chevalier 1999), based on the analysis of the radio light curves (Kulkarni *et al.* 1998). This unusual SN is thought to be associated with GRB 980425 based on spatial and temporal coincidence (Galama *et al.* 1998), as well as its relativistic outflows (Kulkarni *et al.* 1998). However, this GRB, if associated with SN 1998bw (as we believe), releases at least three orders of magnitude less energy in gamma-rays compared to cosmological bursts (Galama *et al.* 1998) such as GRB 011121. So the relation of GRB 980425 to cosmologically located GRBs is unclear. Nonetheless, we make the following curious observation: the γ -ray profile (Figure 1) is of similar duration and smoothness (with a few spikes superposed) as that of GRB 980425.

The current data clearly rule out a jet break on the timescale of the optical data, $t_j \gtrsim 2$ d, and the radio data require $t_j \gtrsim 7$ d. In the formulation of Frail *et al.* (2001) the opening angle of the jet must be wider than $\theta_j > 10$ degrees and hence the true energy release is larger than 5×10^{50} erg. This lower limit is consistent with the the clustering of energies around 5×10^{50} erg found by Frail *et al.* (2001).

Further improvements to the modeling is possible by including the BeppoSAX measurement of the X-ray afterglow (Piro *et al.* 2001); the X-ray flux will pin down ν_c quite well. We also note that the radio fluxes given in Table 2 suffer from strong variability (due to interstellar scintillation). Here we have used the mean fluxes, and in a later paper we intend to report detailed analysis of the scintillation and include the variability as a part of our afterglow modeling, in particular as a way to constrain the size of the afterglow region (c.f. Frail *et al.* 1997).

Thus, at least for one long duration burst the SN-GRB connection and a massive progenitor origin appears to to have been established. However, the true story may be more

complex. The absence of SN components in other GRBs can be explained by appealing to the well known wide diversity in luminosity of Type Ib/c SNe. However, some of the intensively observed afterglows are best modeled by expansion into a homogeneous medium. There could well be two different classes of progenitors within the class of long-duration GRBs (Chevalier & Li 2000).

PAP gratefully acknowledges an Alex Rodgers Travelling Scholarship. GRB research at Caltech (SRK, SGD, FAH, RS) is supported by grants from NSF and NASA. JSB is a Fannie and Hertz Foundation Fellow. RS holds a holds a Senior Fairchild Fellowship. KH is grateful for Ulysses support under JPL Contract 958056, and for IPN support under NASA Grants FDNAG 5-11451 and NAG 5-10710. We thank R. Chevalier for useful discussion. Finally, we thank the staff of Las Campanas Observatory and the ATNF for their assistance, and applaud the heroic efforts of the staff of the AAT in obtaining these observations during the commissioning of IRIS2.

REFERENCES

- Berger, E. *et al.* 2001, ApJ, 556, 556.
- Bloom, J. S. *et al.* 1999, Nature, 401, 453.
- Bloom, J. S., Kulkarni, S. R., Price, P. A., Reichart, D. E., *et al.* 2002, ApJ (submitted), astro-ph/0203391.
- Cardelli, J. A., Clayton, G. C., and Mathis, J. S. 1989, ApJ, 345, 245.
- Chevalier, R. A. and Li, Z. 2000, ApJ, 536, 195.
- Chevalier, R. A. and Li, Z.-Y. 1999, ApJ, 520, L29.
- Eisenhardt, P., Dickinson, M., Standford, S., Ward, J., and Valdes, F. 1999, <http://iraf.noao.edu/iraf/ftp/contrib/dimsumV2/dimsum.readme>.
- Fitzpatrick, E. L. and Massa, D. 1988, ApJ, 328, 734.
- Frail, D. A., Kulkarni, S. R., Nicastro, S. R., Feroci, M., and Taylor, G. B. 1997, Nature, 389, 261.
- Frail, D. A. *et al.* 2001, ApJ, 562, L55.
- Galama, T. J. *et al.* 2000, ApJ, 536, 185.

- Galama, T. J. *et al.* 1998, *Nature*, 395, 670.
- Garnavich, P. M., Holland, S. T., Jha, S., Kirshner, R. P., Bersier, D., and Z., S. K. 2002, GCN Circular 1273.
- Hawarden, T. G., Leggett, S. K., Letawsky, M. B., Ballantyne, D. R., and Casali, M. M. 2001, *MNRAS*, 325, 563.
- Hurley, K., Cline, T., Guidorzi, C., Montanari, E., Frontera, F., and Feroci, M. 2001, GCN Circular 1148.
- Infante, L., Garnavich, P. M., Stanek, K. Z., and Wyrzykowski, L. 2001, GCN notice 1152.
- Kulkarni, S. R. *et al.* 1998, *Nature*, 395, 663.
- Li, Z. and Chevalier, R. A. 1999, *ApJ*, 526, 716.
- MacFadyen, A. I., Woosley, S. E., and Heger, A. 2001, *apj*, 550, 410.
- Olsen, K., Brown, M., Schommer, R., and Stubbs, C. 2001, GCN Circular 1157.
- Persson, S. E. and Murphy, D. C. and Krzeminski, W. and Roth, M. and Rieke, M. J. 1998, *AJ*, 116, 2475.
- Phillips, M., Krisciunas, K., Garnavich, P., Holland, S., Jha, S., Stanek, K. Z., and McCarthy, P. 2001, GCN Circular 1164.
- Piro, L. 2001, GCN Circular 1147.
- Piro, L. *et al.* 2001, GCN 1172.
- Reichart, D. E. 1999, *ApJ*, 521, L111.
- Reichart, D. E. 2001, *ApJ*, 553, 235.
- Sari, R. and Esin, A. A. 2001, *apj*, 548, 787.
- Sari, R., Piran, T., and Halpern, J. P. 1999, *ApJ*, 519, L17.
- Sari, R., Piran, T., and Narayan, R. 1998, *ApJ*, 497, L17.
- Schlegel, D. J., Finkbeiner, D. P., and Davis, M. 1998, *ApJ*, 500, 525.
- Stanek, K. Z. and Wyrzykowski, L. 2001, GCN Circular 1160.
- Stetson, P. B. 1987, *PASP*, 99, 191.

Woosley, S. E. 1993, *ApJ*, 405, 273.

Wyrzykowski, L., Stanek, K. Z., and Garnavich, P. M. 2001, GCN notice 1150.

Table 1. NIR observations of the afterglow of GRB 011121.

Date (2001 UT)	Filter	Magnitude	Telescope
Nov 22.3560	<i>J</i>	17.852 ± 0.045	dP
Nov 22.3573	<i>J</i>	17.730 ± 0.037	dP
Nov 22.3587	<i>J</i>	17.763 ± 0.044	dP
Nov 22.3600	<i>J</i>	17.801 ± 0.040	dP
Nov 22.3614	<i>J</i>	17.821 ± 0.037	dP
Nov 22.3627	<i>J</i>	17.799 ± 0.039	dP
Nov 22.3641	<i>J</i>	17.785 ± 0.035	dP
Nov 22.3654	<i>J</i>	17.770 ± 0.036	dP
Nov 22.3667	<i>J</i>	17.795 ± 0.041	dP
Nov 22.3681	<i>J</i>	17.739 ± 0.038	dP
Nov 22.7177	<i>J</i>	18.352 ± 0.100	AAT
Nov 23.3193	<i>J</i>	19.463 ± 0.068	dP
Nov 28.5	<i>J</i>	21.291 ± 0.282	Baade
Nov 22.3178	<i>K</i>	15.959 ± 0.045	dP
Nov 22.3194	<i>K</i>	15.987 ± 0.040	dP
Nov 22.3211	<i>K</i>	15.908 ± 0.037	dP
Nov 22.3227	<i>K</i>	15.994 ± 0.040	dP
Nov 22.3244	<i>K</i>	15.958 ± 0.040	dP
Nov 22.3263	<i>K</i>	16.002 ± 0.041	dP
Nov 22.3279	<i>K</i>	16.006 ± 0.041	dP
Nov 22.3296	<i>K</i>	16.003 ± 0.039	dP
Nov 22.3296	<i>K</i>	16.003 ± 0.039	dP
Nov 22.3313	<i>K</i>	15.981 ± 0.037	dP
Nov 22.3329	<i>K</i>	16.053 ± 0.039	dP
Nov 22.3349	<i>K</i>	16.039 ± 0.040	dP
Nov 22.3365	<i>K</i>	15.997 ± 0.039	dP
Nov 22.3382	<i>K</i>	16.120 ± 0.041	dP
Nov 22.3398	<i>K</i>	15.996 ± 0.063	dP
Nov 22.3454	<i>K</i>	16.027 ± 0.038	dP
Nov 22.3470	<i>K</i>	16.069 ± 0.036	dP
Nov 22.3487	<i>K</i>	16.100 ± 0.042	dP
Nov 22.3503	<i>K</i>	16.015 ± 0.043	dP
Nov 22.3520	<i>K</i>	16.098 ± 0.043	dP
Nov 22.4771	<i>K</i>	16.421 ± 0.041	AAT
Nov 22.4954	<i>K</i>	16.537 ± 0.041	AAT
Nov 22.5126	<i>K</i>	16.495 ± 0.035	AAT
Nov 22.6066	<i>K</i>	16.605 ± 0.058	AAT
Nov 22.6169	<i>K</i>	16.788 ± 0.042	AAT

Table 1—Continued

Date (2001 UT)	Filter	Magnitude	Telescope
Nov 22.6397	<i>K</i>	16.782 ± 0.038	AAT
Nov 22.6506	<i>K</i>	16.862 ± 0.036	AAT
Nov 22.6612	<i>K</i>	17.019 ± 0.052	AAT
Nov 22.6716	<i>K</i>	16.852 ± 0.039	AAT
Nov 22.6822	<i>K</i>	17.035 ± 0.083	AAT
Nov 22.7272	<i>K</i>	17.005 ± 0.051	AAT
Nov 22.7384	<i>K</i>	17.087 ± 0.079	AAT
Nov 23.3336	<i>K</i>	17.924 ± 0.051	dP
Nov 28.7092	<i>K</i>	19.346 ± 0.234	AAT

Note. — (a) Observations at the du Pont (dP) 2.5-m were made by K. Koviak; observations at the AAT were made by S.D. Ryder (Nov 22) and K. Gunn (Nov 28); observations at the Baade telescope were made by M. Phillips. (b) The following reference stars were used. For K_s observations on the AAT we observed UKIRT Faint Standards FS 7, 11 and 13 (Hawarden *et al.* 2001) on 2001 Nov. 28. SJ9113 (Persson, S. E. and Murphy, D. C. and Krzeminski, W. and Roth, M. and Rieke, M. J. 1998) was observed at the du Pont telescope on 2001 Nov. 23. We assumed an atmospheric extinction coefficient of 0.09 mag/airmass in *K* for the du Pont observations, and that the colour terms were negligible. We used the reference stars calibrated by Phillips *et al.* (2001) to calibrate our *J*-band observations. (c) The AAT measurement of Nov. 28th is contaminated both by the host and the nearby star.

Table 2. Radio Observations of GRB 011121 made with the Australia Telescope Compact Array.

Epoch (UT)	ν_0 (GHz)	$S \pm \sigma$ (μJy)
2001 Nov 25.20	4.80	240 ± 70
2001 Nov 28.64	4.80	510 ± 38
2001 Dec 6.80	4.80	350 ± 42
2001 Dec 15.80	4.80	250 ± 34
2001 Dec 22.90	4.80	-99 ± 49
2002 Jan 23.85	4.80	320 ± 38
2001 Nov 22.83	8.70	210 ± 40
2001 Nov 25.08	8.70	450 ± 130
2001 Nov 28.64	8.70	610 ± 39
2001 Dec 6.80	8.70	220 ± 58
2001 Dec 15.80	8.70	274 ± 37
2001 Dec 22.90	8.70	237 ± 46
2002 Jan 23.85	8.70	-99 ± 47

Note. — The columns are (left to right), UT date of the start of each observation, center frequency, and peak flux density at the best fit position of the radio transient, with the error given as the root mean square noise on the image. All observations were obtained using the continuum mode and a 128 MHz bandwidth. Flux calibration was performed using PKS B1934–638, while the phase was monitored using PKS B1057–797.

Table 3. Afterglow Model Testing

Model	ν_c	(b, c)	Closure	p
ISM	B	$(-3/2, 0)$	1.04 ± 0.47	3.21 ± 0.08
ISM	R	$(-3/2, 1/2)$	2.04 ± 0.47	2.88 ± 0.08
Wind	B	$(-3/2, -1/2)$	0.04 ± 0.47	2.55 ± 0.08
Wind	R	$(-3/2, 1/2)$	2.04 ± 0.47	2.88 ± 0.08
Jet	B	$(-2, -1)$	-0.86 ± 0.31	1.66 ± 0.06
Jet	R	$(-2, 0)$	0.14 ± 0.31	1.66 ± 0.06

Note. — Calculation of the closure relations $\alpha + b\beta + c$ for a variety of afterglow models. A successful model will have a value of zero for the closure relation. The ISM and Wind models are for isotropic expansion in an homogeneous and wind-stratified medium respectively. The Jet model is for collimated expansion, with the jet break time before the first observations were made. The relations are dependent on the assumed location of the cooling frequency, ν_c relative to the optical and NIR bands, ν_O : the case $\nu_c > \nu_O$ is denoted by “B” (for blueward) and $\nu_c < \nu_O$ by “R” (for redward). p is the electron energy power law index.

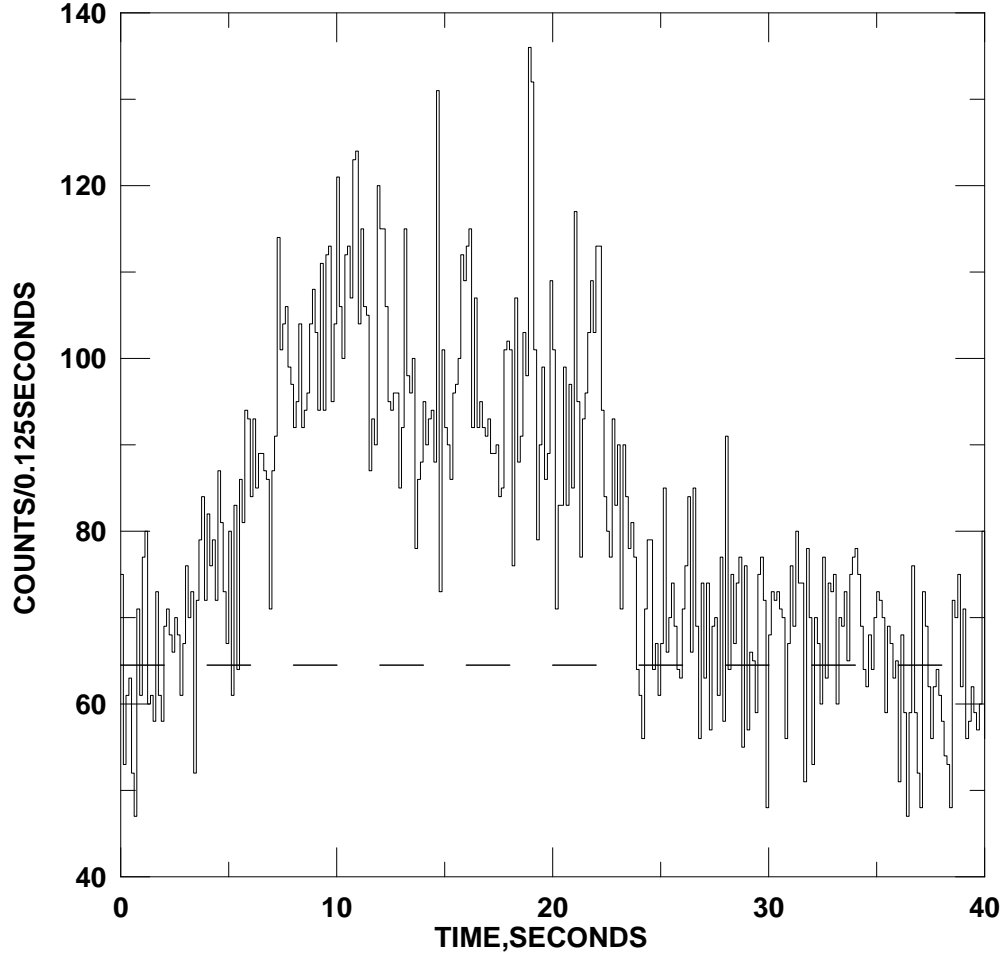


Fig. 1.— Time history of GRB 011121 in the 25-150 keV energy range, as observed by Ulysses. The dashed line gives the background rate. Zero on the time axis corresponds to an Earth-crossing time of 67630.899 s.

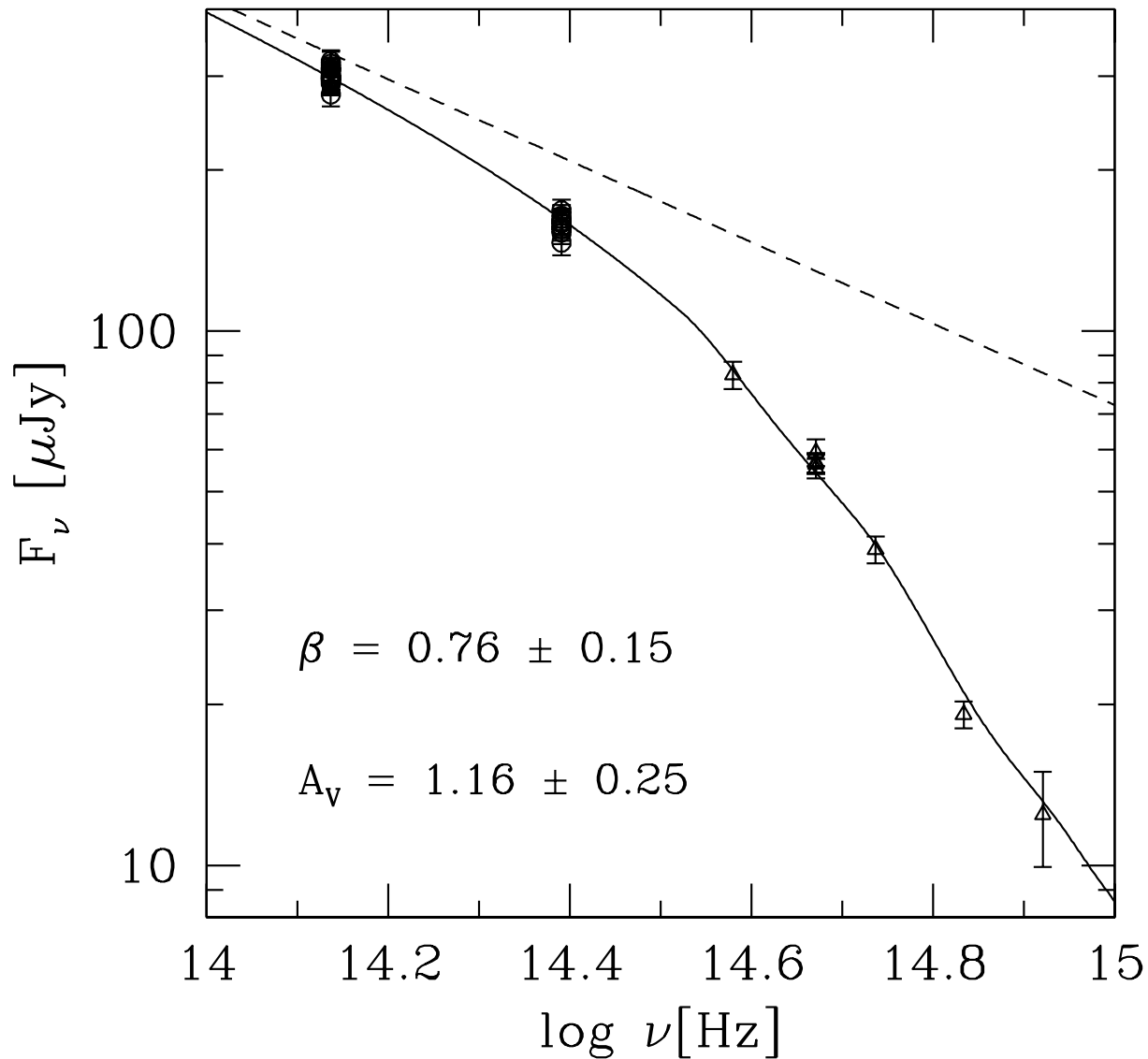


Fig. 2.— The optical and NIR spectral flux distribution of the afterglow of GRB 011121 at 0.5 d, based on measurements presented here (circles) and from the literature (triangles; Olsen *et al.* 2001; Stanek & Wyrzykowski 2001). Measurements taken within 0.5 ± 0.1 d have been transformed to 0.5 d using the best fit model. The solid lines indicates our best fit to the data, using a power-law model plus foreground extinction. The dashed line is the intrinsic spectrum of the afterglow.

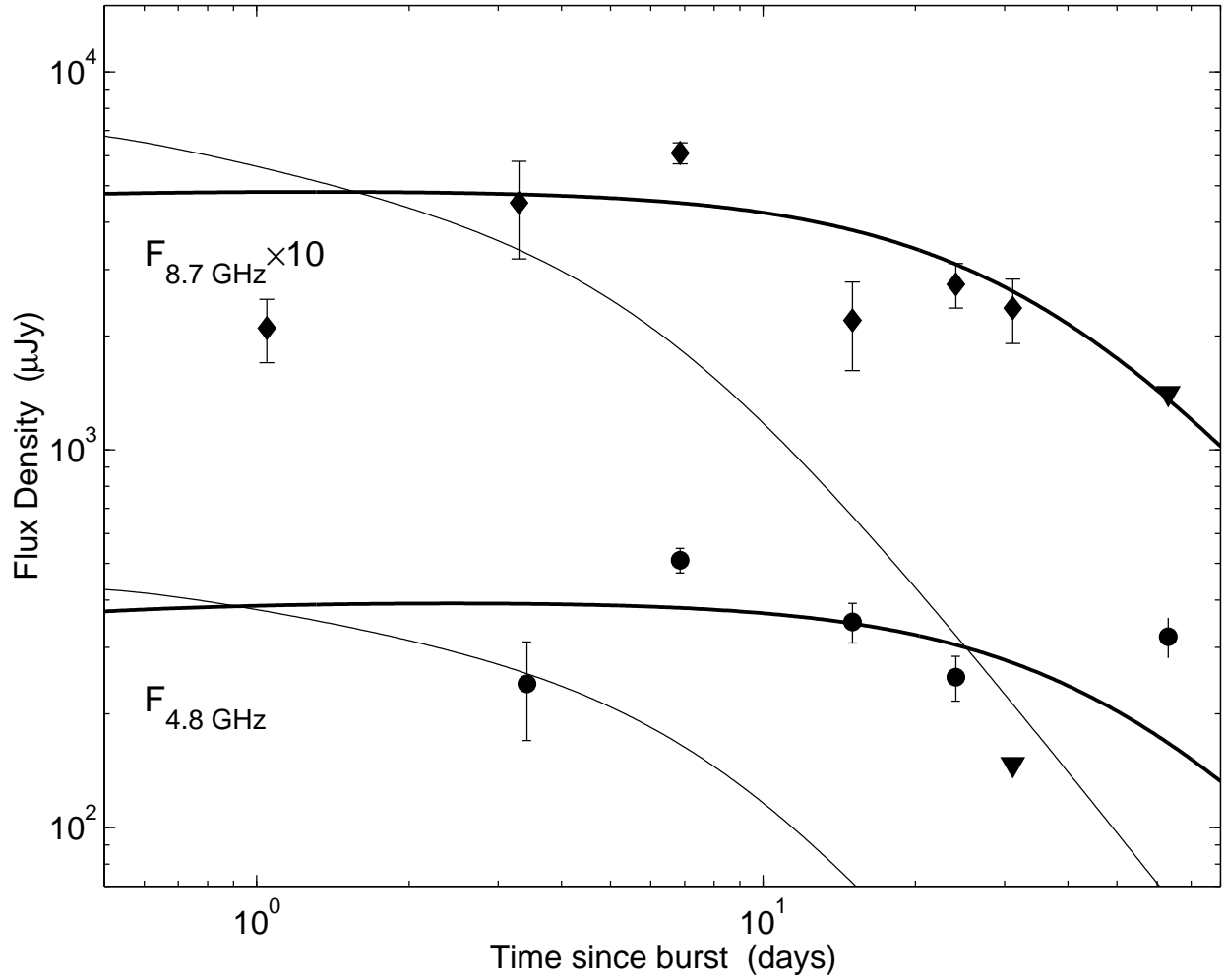


Fig. 3.— The radio light curve of the afterglow of GRB 011121. The solid line is our wind model, the thin line is a representative jet model, which is clearly excluded by the data. The radio data exhibit strong modulation due to interstellar scintillation and, as a result, deviate from our model by more than 1σ . This will be addressed in a future paper.

